*Plant Pathol. J. 38(4) : 372-382 (2022)*
https://doi.org/10.5423/PPJ.OA.05.2022.0067
eISSN 2093-9280

Research Article Open Access

The Plant Pathology Journal


# Microbiota Communities of Healthy and Bacterial Pustule Diseased Soybean

**Da-Ran Kim[1]*, Su-Hyeon Kim[2], Su In Lee[2], and Youn-Sig Kwak [1,2]***

[1]*Research Institute of Life Science, Gyeongsang National University, Jinju 52828, Korea*
[2]*Division of Applied Life Science (BK21Plus), Gyeongsang National University, Jinju 52828, Korea*

*(Received on May 10, 2022; Revised on June 27, 2022; Accepted on June 29, 2022)*

**Soybean is an important source of protein and for a wide range of agricultural, food, and industrial applications. Soybean is being affected by *Xanthomonas citri* pv. *glycines*, a causal pathogen of bacterial pustule disease, result in a reduction in yield and quality. Diverse microbial communities of plants are involved in various plant stresses is known. Therefore, we designed to investigate the microbial community differentiation depending on the infection of *X. citri* pv. *glycines*. The microbial community's abundance, diversity, and similarity showed a difference between infected and non-infected soybean. Microbiota community analysis, excluding *X. citri* pv. *glycines*, revealed that *Pseudomonas* spp. would increase the population of the infected soybean. Results of DESeq analyses suggested that energy metabolism, secondary metabolite, and TCA cycle metabolism were actively diverse in the non-infected soybeans. Additionally, *Streptomyces bacillaris* S8, an endophyte microbiota member, was nominated as a key microbe in the healthy soybeans. Genome analysis of *S. bacillaris* S8 presented that salinomycin may be the critical antibacterial metabolite. Our findings on the composition of soybean microbiota communities and the key strain information will contribute to developing biological control strategies against *X. citri* pv. *glycines*.**

***Keywords*** **:** biotic stress, microbial community, *Streptomyces*, *Xanthomonas citri* pv. *glycines*

*Co-corresponding authors.
D.-R. Kim
Phone) +82-55-772-1922, FAX) +82-55-772-1929
E-mail) dalan0125@gnu.ac.kr
Y.-S. Kwak
Phone) +82-55-772-1922, FAX) +82-55-772-1929
E-mail) kwak@gnu.ac.kr
ORCID
Y.-S. Kwak
https://orcid.org/0000-0003-2139-1808

*Handling Editor* : Hyun Gi Kong



According to the Organization for Economic Cooperation and Development (OECD), the world will be demanding more food than the amount of productivity of crops in the near future (Jägermeyr et al., 2020; Xu et al., 2019b). By 2050, the world's population will reach 9.7 billion, and the food supply will face difficulties due to reduced crop productivity (Chen et al., 2016; Jägermeyr et al., 2020; Lau et al., 2017; Rodriguez and Durán, 2020). These issues increased the request for a second green revolution in agriculture. They led to the emergence of the concept of the plant microbiome and promoted research activity in related fields (Reverchon and Méndez-Bravo, 2021). The plant microbiome has all surrounded factors to protect well-grown plants, such as microbe factors mutually interacting in a beneficial direction (Dini-Andreote and Raaijmakers, 2018; Xiong et al., 2021). All the plant-associated microorganisms are expanded from soil to flower. Also, their living spaces are categorized as below-ground: rhizosphere, root episphere, root endosphere, and above-ground: episphere, endosphere, anthosphere, and seed (Bintarti et al., 2022; Hannula et al., 2019; Kim et al., 2019a, 2019b; Lu et al., 2018; Simonin et al., 2022).

The soybean is the most important crop for providing protein, and the crop is known for being essential for a wide range of agricultural, food, and industrial applications. Also, it is the world's most cultivated annual herbaceous legume (Jeong et al., 2019). However, the primary crop has been faced with the loss of productivity by climate

change and increased damage caused by various disease occurrences. Among diseases in soybean, root rot disease caused by *Fusarium solani*, is the most devastating disease. Interestingly, nodulation root by *Rhizobia* showed less damage by the fungal pathogen (Ikeda et al., 2008). Research on microbiota communities has been conducted with soybeans, and the diversity of microbiota is known to contribute to ensuring healthy and high-quality soybean productivity (de Almeida Lopes et al., 2016). Rhizospheric microbes demonstrate crucial roles in shaping rhizobia-host interaction. For example, *Bacillus* groups regulate the growth of sinorhizobia and bradyrhizobia and promote nodulation under saline-alkali conditions (Han et al., 2020). Endophytic bacteria *Acinetobacter*, *Variovrax*, *Burkholderia*, and *Pseudomonas* species are associated with field-grown soybean (de Almeida Lopes et al., 2016). In general, endophyte microbes have more dependent on the host plant (Mingma et al., 2014). Bacterial endophytes are inhabitants inside the plant tissue, and these provide beneficial mechanism roles that prevent pathogen infection and promote host growth (Orozco-Mosqueda and Santoyo, 2021; Xiong et al., 2021). Also, the symbiotic relationship between endophytes provides various secondary metabolites to the host plant (Dang et al., 2020). Despite consistent evidence of the beneficial microbe interaction with the host, it is remained a challenge to identify host genetics and plant microbiome composition (Deng et al., 2021). The diversity and composition of bacterial endophytes are typically studied with high-throughput sequencing methods to explain the microbial community levels (Bintarti et al., 2022). Endophytic communities provide tolerances toward heavy metals, pollutants, and high salinity stresses (Dong et al., 2018; Han et al., 2020; Kim et al., 2021b; Longley et al., 2020; Reverchon and Méndez-Bravo, 2021).

*Xanthomonas citri* pv. *glycines*, the bacterial pustule disease pathogen, causes a decrease in soybean production and quality worldwide (Kang et al., 2021). The pathogen is infected through natural openings or wounds in plants. To understand and develop control methods for the disease, we need to investigate a piece of microbial ecological information in microbial interaction. However, soybean-associated microbial communities have been rarely studied. Therefore, we investigated the microbiota communities' structure between infected and non-infected soybean and changes in the abundance of the keystone taxa. Additionally, we also analyzed the genome of a key strain, which contributes to suppressing the bacterial pustule disease pathogen.

## Materials and Methods

**Plant growth condition.** To sterilize, 3 g of soybean seeds (*Glycine max* cv. Daewon) were transferred into a 50-ml tube, then added 70% ethanol for 30 s. After shaking, the supernatant ethanol was discarded, added 1% NaOCl and vortexed for 30 s. After these steps, the seeds were washed with dd$H_2O$ for 2 min, and the washing was repeated three times then, the seeds were placed on a sterilized cotton paper in a petri dish. The plates were incubated for 3 days at 28°C in dark conditions. The germinated seeds were replaced in a plastic squire pot (18 cm × 18 cm). Each pot has more than 20 cm of distance to prevent cross-contamination. The plants were grown in a glass greenhouse, in which conditions were light for 14 h, 28 ± 3°C and dark for 10 h, 15 ± 3°C for 28 days, respectively.

**Bacterial inoculation and disease indexing.** *X. citri* pv. *glycines* was streaked on PDK agar (peptone [Difco, Franklin Lakes, NJ, USA] 10 g, potato dextrose [Difco] 10 g per liter), and a single colony was inoculated in 10 ml PDK broth and incubated for 3 days at 28°C. The cultured cells were added to 100 ml of PDK broth for 3 days at 28°C. Whereas infected and non-infected treatments were separated by the small greenhouse (length: 5 m), and the pathogen stock ($10^6$ cfu/ml) was sprayed on the soybean leaves. Ten days after the inoculation, the pathogen occurred symptoms on the leaves and 5 levels of index evaluated the disease severity; 0, no symptom; 1, less than 10-15 small yellow or brown spots; 2, more than 0.5 cm browning area; 3, darkening and browning area more than 30%; 4, darkening and browning area more than 50%; 5, death (Kang et al., 2021). Non-infected and infected plants were separated into two small greenhouses (3 m × 1.5 m) and the disease index ($n = 28$) was measured with an independent student's *t*-test ($P = 0.05$).

*Xanthomonas citri* pv. *glycines* was re-isolated from the infected soybean leaves, which appeared in disease index value 4. The leaves were cut into 5 mm × 5 mm, sterilized with 70% ethanol for 30 s, 1% NaOCl for 30 s, and washed twice with distilled water. The leaves were inoculated on 1/5 TSA medium (tryptic soya broth 30 g, agar 20 g per liter) at 28°C for 3 days. Colonies growing near the leaves were streaked to another TSA medium for pure culture and extraction of genomic DNA of the pathogen. Genomic DNA was prepared by cetyltrimethylammonium bromide (CTAB) method (Wilson, 2001). For sequencing of the pathogen, the upstream region of the hypothetical protein gene was amplified using XGF (5'-TGTGCGGC-

CAGTAGATAGTGAGC-3'), XGR (5'-CCGAGGGC-CAGCAAAGAAG-3') primer pairs (Park et al., 2007). Polymerase chain reaction (PCR) reaction was carried out with a total of 20 µl of a mixture (1 µl of genomic DNA, 1 µl of each primer [10 pmol], 2 µl of 10× Reaction buffer, 1 µl of dNTPs [10 mM], 0.5 µl of Taq DNA polymerase [500 U; Bioneer, Daejeon, Korea]). The cycling condition was followed: 94°C for 10 min (1 cycle), 94°C for 1 min, 62°C for 30 s, 72°C for 1 min (25 cycles), 72 °C for 10 min by a T100 thermal cycler (Thermo Fisher, Waltham, MA, USA). The PCR products were purified using Expin Gel SV kit (Bioneer), and sequencing was carried out by Macrogen (Seoul, Korea). The sequencing was aligned with the nucleotide BLAST search program (https://blast.ncbi.nlm.nih.gov/Blast.cgi) in NCBI (National Center for Biotechnology Information). The phylogenetic tree was analyzed using GenBank BLAST with the maximum likelihood algorithm in the MEGA 10 program.

**DNA extraction, metagenome, and analysis of microbial community.** After 27 days of *X. citri* pv. *glycines* inoculation, the non-infected and the infected soybeans rhizosphere, root endosphere, and stem endosphere samples were harvested. The root or stem tissues contained a 50-ml conical tube was filled with 1× phosphate buffered saline (PBS) buffer (10× PBS: 80 g of NaCl, 2 g of KCl, 1.44 g of $Na_2HPO_4$, 2.4 g of $KH_2PO_4$, adjusted to a pH of 7.4 and a final volume of 1 liter) and was sonicated at 35 kHz for 15 min (Kim et al., 2019a). The sonicated samples were sterilized in 70% ethanol for 30 s, 1% NaOCl for 30 s, washed with $ddH_2O$ several times, and then air-dried under a sterilized hood for 30 min. For DNA extraction, 0.5 g of tissue was used. The extraction protocol of FastDNA SPIN Kit (MP Biomedicals, Irvine, CA, USA) followed the manufacturers' instructions.

For amplification of the V4 region in 16S rRNA, DNA was diluted to 8 ng/µl and amplified using 515F (5'-GTGCCAGCMGCCGCGGTAA-3'), 805R (5'-GACTACHVGGGTATCTAATCC-3'), which is including overhang adapter sequences, PNA probes (pPNA, mPNA) (Lundberg et al., 2013) to block plant-derived mitochondrial and chloroplast DNA. The PCR reaction was conducted with 2.5 µl of DNA, 1 µl of each primer (10 pmol), 2.5 µl of each PNA probe (7.5 µM), 12.5 µl of KAPA HiFi HotStart ReadyMix (Roche, Basel, Switzerland) in the final volume of 22 µl. The PCR condition followed: 95°C for 3 min (1 cycle), 95°C for 30 s, 78°C for 10 s, 55°C for 30 s, 72°C for 30 s (25 cycles). The PCR amplicons were purified using AMPure XP (Beckman Coulter, Brea, CA, USA). The amplicons were loaded on 0.8% agarose gels in electrophoresis with 100 V for 20 min (Mupid ExU, Tokyo, Japan) to confirm the amplicon size. Metagenome sequencings were performed with Illumina Miseq by Macrogen.

The raw sequence was analyzed by utilizing the DADA2 software package (Callahan et al., 2016) version 1.8 guidelines (https://benjjneb.github.io/dada2/tutorial_1_8.html) in R version 4.1.3. Libraries were truncated to 265, 215 more than 30 quality scores, merged with forward, reverse reads, and removed chimera sequences. Amplicon sequnce variant (ASV) was assigned to taxonomy by Silva (https://www.arb-silva.de/download/arb-files/) and IDTAXA (Murali et al., 2018), appearing cutoff at 97% similarity. Analyses of richness and evenness were conducted by ggiNEXT (version 2.0.20) and pyloseq (version 3.15). Principal coordinates analysis (PCoA) was shown to visualize using Bray-Curtis dissimilarity. Pathway analyses were conducted by DESeq version 3.14 to normalize the fold change value of relative abundance and PiCRUSt2 version 1.1.4 predicted the data to the functional potential of a bacterial community on based their 16s RNA identity ($P_{adj} < 0.05$), and graph visualization was performed by ggplot2 version 3.3.5. Kruskal-Wallis test was used for statistical analysis ($P = 0.05$) (Kruskal and Wallis, 1952).

**Genome annotation and re-classification of *Streptomyces bacillaris* S8.** Genome sequencing of *Streptomyces* sp. S8 was performed using the Pacific Biosciences RSII platform (Macrogen) (Jeon et al., 2019). The genome of S8 was re-analyzed and annotated in this study; average nucleotide identity (ANI) with EzBioCloud (Yoon et al., 2017), classification of gene functions by Prokka (v 1.14.6), and the genome were annotated by rapid annotation using subsystem technology 2.0 (RAST 2.0) (Aziz et al., 2008). The classic RAST was set as the default condition, and it functioned by turning on the bacterial domain and automatically fixed error options. A genome map was drawn by ggplot2 (3.3.5) in R (4.1.3 version) based on the Prokka results. The genome information was transformed from gff format to data frame object. GC ratio and GC skew were calculated and plotted by bar graph inner circle in total level and per 10,000 bp. Coding sequence was indicated as a line, and tRNA or mRNA was represented by a black dot in the out circle. Putative secondary metabolites were predicted by antiSMASH bacterial version 6.0 (Blin et al., 2021), in which antimicrobial-related compounds biosynthesis genes were identified in *S. bacillaris* S8. 16S rRNA gene-based phylogenetic analysis was also performed with a maximum likelihood method. The phylogenetic tree was constructed by the MEGA 11 program. Alignment muscles were a gap opening penalty of 15.00 and a gap extension

penalty of 6.66. Bootstrap values were obtained after 1,000 re-samplings for each node, and the Jukes-Cantor model was using calculated for the distance.

**Antibacterial activity.** Three different antibiotics (Sigma-Aldrich, St. Louis, MO, USA), sallinomycin (≥98%), bafillomycin A (≥90%), and valinomycin (≥99%) were tested for antibacterial effects with a two-layer method (Kim and Kwak, 2021). Solvent conditions were followed: valinomycin in dd$H_2O$, salinomycin, and bafilomycin in chloroform, and each antibiotic was prepared with three different concentrations as 10 µg/ml, 50 µg/ml, and 100 µg/ml. The antibiotic solution was inoculated on a filter disk (0.8-mm diam.) and each disk was received 20 µl of the antibiotic and dried for 20 min at room temperature then *X. citri* pv. *glycine* was overlaid. The pathogen was cultured in PDK broth (peptone [Difco] 10 g, potato dextrose [Difco] 10 g per 1 liter) for 3 days at 28°C, then 10-ml cultured bacteria were added in 40-ml of pre-cooled 0.2% carrageenan and overlaid onto the antibiotic plates. The plates were dried for 1 h, incubated at 28°C for 3 days and a clean zone around the disk determined the antibacterial inhibition rate. The pathogen growth inhibition assay was repeated 8 times and Kruskal Rank Sum followed by Tukey's honestly significant difference ($P = 0.05$) was used for mean separation.

## Results and Discussion

**Comparison of microbiota diversity between *X. citri pv. glycines* infected and non-infected soybean.** Microbial communities are significantly contributing to plant health and growth related to the sustainability of agriculture (Dini-Andreote and Raaijmakers., 2018; Xiong et al., 2021). Soybean rhizosphere and endosphere microbiota communities can be changed by various factors such as nodulation, pathogen infection, or genotype of the plant (Han et al., 2020). In this study, we explored the effects of *X. citri pv. glycines* infection on soybean microbiota community struc-

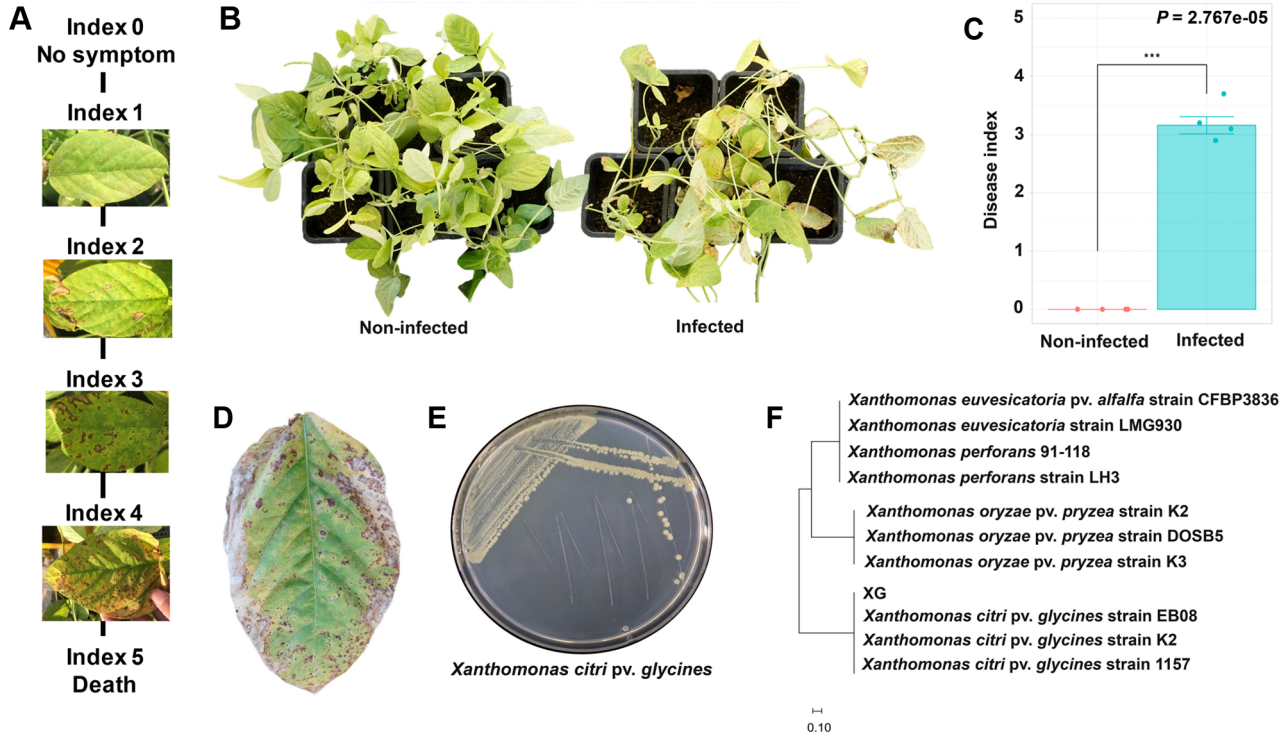


**Fig. 1.** Bacterial pustule disease caused by *Xanthomonas citri* pv. *glycines.* For disease occurrence *X. citri* pv. *glycines* was cultured in 1/5 PDK broth medium for 5 days. The cultured bacteria were adjusted to $OD_{600}$ 0.3 ($10^6$ cfu/ml) and sprayed on the leaves of soybeans with a sprayer. After 30 days of inoculation, the severity of bacterial pustule disease was measured using the disease index ($n = 28$). (A) The disease index value of the soybean bacterial pustule, caused by *X. citri* pv. *glycines*. (C) The disease indexes showed a statistical difference according to the treatment groups using the Wilcoxon rank-sum test. (B, D, E) Re-isolation and identification of *X. citri* pv. *glycines*. Soybean leaves were sterilized and inoculated on 1/5 TSA medium of 28°C for 3 days. (F) Phylogenetic tree of the region of the hypothetical protein (400 bp) in *X. citri* pv. *glycines,* the tree was generated with the maximum likelihood algorithm of the MEGA 11 program.


**Fig. 2.** Diversity and abundance of bacterial communities in soybean rhizosphere, root endosphere, and stem endosphere. Relative abundance was analyzed at the family level and cutoff in the top 10 ($n = 28$). (A) Relative abundance between infected and non-infected by *X. citri* pv. *glycines*. The ratio of Xanthomonadaceae was low at root and rhizosphere in the untreated group. (B) Relative abundances were recalculated after the removal Xanthomonadaceae.

tures. The pathogen-infected soybean appeared with yellow spots and browning areas on the left as disease symptoms and re-isolated the pathogen identified as *X. citri* pv. *glycines* (Fig. 1).

Soybean plants were divided into 3 sections: rhizosphere, root endosphere, and stem endosphere for microbiota investigation. 10,425,683 reads and 6,752 sequences were identified in the rhizosphere, root endosphere, and stem endosphere. All data shows 100 % in Good's coverage and Chao's coverage. Total observed ASV was 6,752 and alpha diversity in observed level was a minimum 100 to a maximum 867, Shannon index level was lowest in the stem to 1.3-1.5 and highest was 6 at rhizosphere samples (Fig. 2). In the infection soybean, microbial diversity was decreased by enrichment of Xanthomonadales and Enterobacterales (Fig. 2). But the non-infection soybean was well constructed with microbial communities and presented many bacterial taxa. In the rhizosphere, the alpha diversity of the infected soybeans was lower than the non-infected plants, and the beta diversity was significantly different between the infected and the non-infected soybeans ($P_{adj} = 0.001$) (Figs. 3 and 4). There was no difference in the alpha diversity in the root endosphere, but the pathogen infection affected the beta diversity ($P_{adj} = 0.001$) (Figs. 3 and 4). Microbiota at the stem endosphere, alpha diversity, and beta diversity showed a difference in accordance with the disease. At the order level, 20-80% of the total population was Xanthomonadales in the infected stem endosphere. However, root endosphere and rhizosphere microbiota had no dramatic increases in Xanthomonadales (Fig. 2A). The

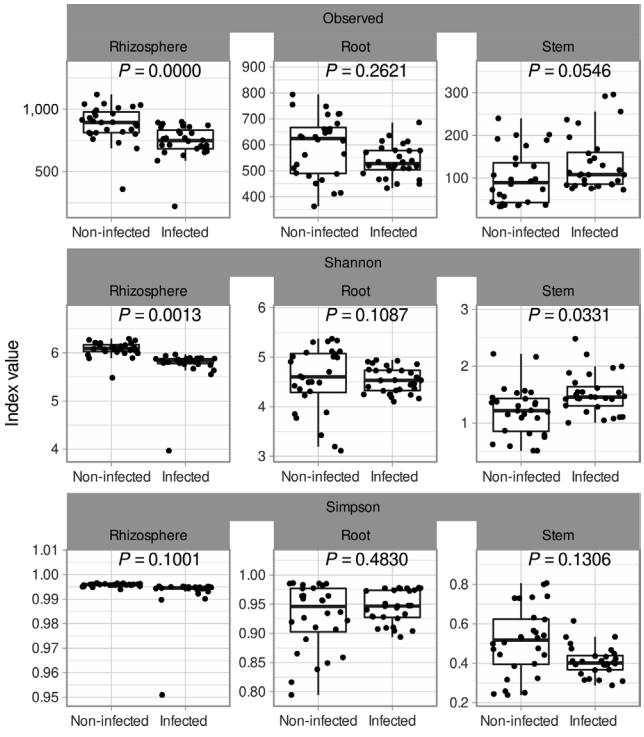


**Fig. 3.** Species richness and diversity of *Xanthomonas citri* pv. *glycines* infected and non-infected soybean. The bacterial taxa were assigned by ID-TAXA, which was machine-learned to confidence in identifying with SILVA 138 SSU. Variables (Observed, Shannon, and Simson) were used alpha diversity. *P*-value indicated Wilcoxon signed-rank test and removing outlier based on IQR method.

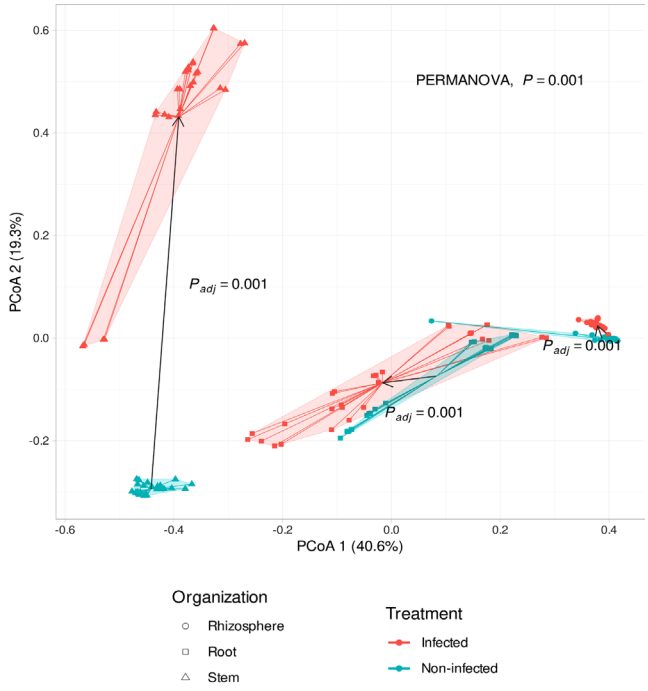


**Fig. 4.** Principal coordinates analysis (PCoA) to visualize similarities or dissimilarities between *Xanthomonas citri* pv. *glycines* infected and non-infected soybean based on Bray-Curtis distance. Statistical analysis was conducted by permutational analysis of variance (PERMANOVA). Shapes of samples appeared organized (rhizosphere, root, stem).

non-infected soybean rhizosphere and root endosphere had similar bacterial communities in top order levels that listed Burkholderialses, Rhizobiales, Chitinophagales, Saccharimonadales, Streptomycetales, Pedosphaerales, Corynebacterialse, Caulobacterales, and Enterobacterales (Fig. 2A). These taxa had a lower abundance at the stem endosphere than the rhizosphere and the root endosphere. Burkholdelaes, Streptomycetes, and Rhizobiales showed more abundance in the stem endosphere of the non-infected soybean. In the infected plant, the rhizosphere and the root endosphere had less changed the microbial community composition. Many types of research presented three microbes crucial role in plant endophytes to against pathogen attack, drought salinity, and growth promotor on their host (Colombo et al., 2019; Hwang et al., 2021; Lopez-Velasco et al., 2013; Xu et al., 2019a). But the stem endosphere had dramatically increased the abundance of Xanthomonadaceae and Pseudomonadales. After excluding Xanthomonadales from the communities (Fig. 2B), Enterobacterales was the most abundant taxa in the infected stem endosphere of soybean (Fig. 2B).

PCoA results presented that microbial community structures were affected by the bacterial pustule pathogen infection ($P_{adj}$ = 0.001). According to the pathogen's infection, the stem endosphere microbiota was the most significantly affected (Fig. 4). The distance of microbiota communities in root and stem by treatment of *X. citri* pv. *glycines*, it can be found that the microbiota of each tissue is different. In the stem of infected and non-infected soybean, microbial communities were not similar, especially Xanthomonadaceae dominated in the infected soybean stem endosphere. It was presumed that the treatment of *X. citri* pv. *glycines* on the leaves moved to the stem endosphere. However, except for Xanthomonadaceae from the community in the *X. citri* pv. *glycines* infected soybean, the population of Pseudomonadaceae increased in all tissues compared with the non-infected plants. This may result from the genetic similarity between Xanthomonadaceae and Pseudomonadaceae because of the limitations of the pyrosequencing that was analyzed with a limited region of 16S rRNA sequencers (Teeling and Glockner, 2012). Therefore, it may require proceeding with an in-depth phylogenetic analysis along with the previous analysis.

Next, we compared the abundance of taxonomic taxa

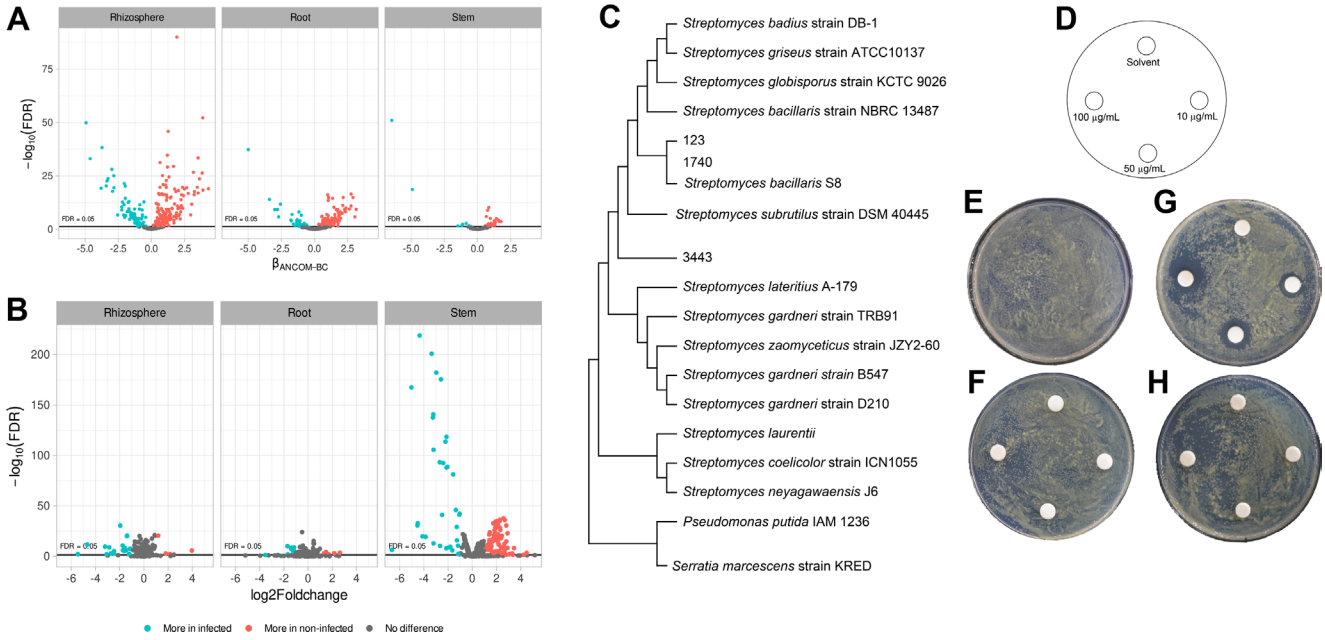


**Fig. 5.** Differences in the abundance of taxa and pathways between the groups. (A) Volcano plot of residuals between infected and non-infected soybean and estimated with taxa family level. (B) Metabolite pathway expression in bacterial community confirmation using PICRUt2 package version 2.3.0. (C) Phylogenetic tree between *Streptomyces bacillaris* S8 and *Streptomyces* sq no. 123, 1740, and 3443 at 16S rRNA region with alignment muscles and MEGA 11 program. (D-H) Antibacterial activity of antibiotics: control (E), valinomycon (F), salinomycin (G), Bafilomycin (H). *X. citri* pv. *glycines* spread on PDK agar media by $OD_{600}$ = 0.3 ($10^7$ cfu/ml) and added filter disk (0.8 mm). Plates were cultured at 28°C for 3 days.

by Analysis of Compositions of Microbiomes with Bias Correction (ANCOMBC). As a result, 159 taxa for rhizosphere, 110 taxa for root endosphere, and 40 taxa for stem endosphere were listed as more abundant in the non-infected soybean. The taxa were Actiomycetaceae, Acidobacteriaceae, Acetobactereaceae, and Burkholderiaceae (Fig. 5A). The most abundant Actiomycetaceae taxa in the non-infected soybean were ASV-123, ASV-1740, and ASV-3443. The ASV-123 and the ASV-1740 showed 99% similarity with *S. bacillaris* S8 isolated from turfgrass rhizosphere and showed exceptional antibiotic activity (Jeon et al., 2019) (Fig. 5C). And PiCRUSt results suggested that microbiota in the non-infected soybean highly expressed defense mechanisms and carbon metabolism for a bacterial living related metabolic pathway (Fig. 5B). Bacterial carbon and nitrogen sources may be degraded in the stem by lactose and galactose degradation processes, fucose and rhamnose degradation, and sulfolactate degradation composed of the TCA cycle as energy-generating mechanisms (Table 1). And aclacinomycin biosynthesis, osmotic, and heat stress adaptation pathways were also significantly activated (Table 1). Other groups were geranylgeranyl diphosphate biosynthesis, UDP-2,3-diacetamido-2,3-dideoxy-α-D-mannuronate biosynthesis (Table 1), that have known as conducting bacterial immune system (Teheran-Sierra et al., 2021). In the metabolite pathway, the non-infected soybeans microbiota community had many energy metabolite pathways such as lactose, galactose, fucose, rhamnose degradation. Lactose and galactose degradation at the cleavage of glucose and fucose is a six-carbon sugar found in N-linked glycans on the plant cell surface, and the L-fucose can be used complete source of energy (Villalobos et al., 2015). Also, other pathways are rolled to protect the host, TCA cycle in energy mechanisms, osmotic, and heat stress adaptation pathways. *Streptomyces* produce secondary metabolite, which is aclacinomycin biosynthesis. These pathways were more active in the non-infected soybean microbiota community than in the infected plant. The finding suggested that the microbiota community was well-established in healthy soybeans.

**Genome analysis and antibacterial activity of *S. bacillaris* S8.** ASV-123, ASV-1740, and ASV-3443 were abundant in healthy soybean stem endosphere, and 16S rRNA phylogenetic results suggested that the ASVs were matched to *Streptomyces* sp. S8 (Jeon et al., 2019). The strain was re-classified with whole-genome sequences result by Ez-BioCloud (Yoon et al., 2017), which showed 98% ANI

**Table 1.** Metabolic pathways of endophyte microbiota community in the non-infected soybean

| Category | Subcategory | metaCYC_id | Fold change (Log 2) | $P_{adj}$ |
|---|---|---|---|---|
| Fucose and rhamnose catabolism | Fucose and rhamnose degradation | FUC-RHAMCAT-PWY | 2.399 | 0.020090822 |
| Lactose catabolism | Lactose and galactose degradation I | LACTOSECAT-PWY | 2.368 | 0.039069593 |
| Glutamate catabolism | L-glutamate degradation | P162-PWY | 4.226 | 0.030687106 |
| TCA cycle | L-glutamate degradation VIII (to propanoate) | PWY-5088 | 3.073 | 0.007388114 |
| | Reductive TCA cycle II | PWY-5392 | 1.707 | 0.001297049 |
| | Glutaryl-CoA degradation | PWY-5177 | 4.270 | 0.035996333 |
| Peptidoglycan | Peptidoglycan biosynthesis V (beta-lactam resistance) | PWY-6470 | 2.306 | 0.002320119 |
| | Peptidoglycan biosynthesis IV | PWY-6471 | 2.312 | 0.001255018 |
| Glycolysis | Propanediol degradation - Try-panocyc | PWY-7013 | 1.915 | 0.005707176 |
| Secondary metabolites by *Streptomyces* | Aclacinomycin biosynthesis | PWY-7354 | 2.767 | 0.030687106 |
| Response to heat stress | Isoprene biosynthesis II | PWY-7391 | 1.243 | 0.045515622 |
| Osmotic adaptation | Mannosylglycerate biosynthesis I | PWY-5656 | 3.362 | 0.024474646 |
| Vitamin biosynthesis | Biotin biosynthesis II | PWY-5005 | 2.602 | 0.01178234 |

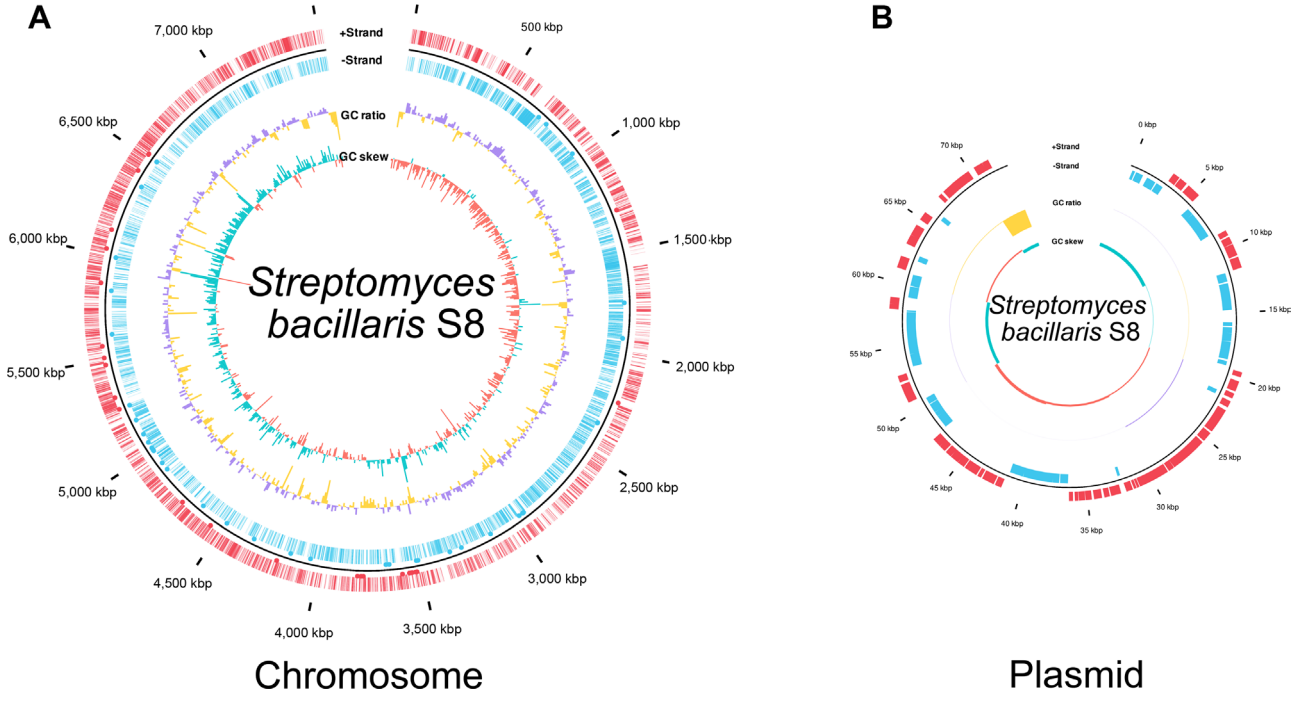


**Fig. 6.** *Streptomyces bacillaris* S8 genome reassigned with genome map. (A) *S. bacillaris* S8 chromosome. (B) Plasmid of *S. bacillaris* S8. The genome map was drawn by annotation result in Prokka v1.14.6. Marked characteristics are shown from outside to the center; coding sequence (CDS) on forwarding strand (+), CDS on reverse strand (–), GC content, and GC skew. The genome map was drawn using the ggplot2 package of the R (v4.0.3).

**Table 2.** Classification of *Streptomyces bacillais* S8 based on genome and selected gene sequences

| Hit taxon | ANI (%) | Accession no. | 16S rRNA (%) | *recA* (%) | *rplC* (%) |
|---|---|---|---|---|---|
| *Streptomyces bacillaris* | 95.31 | GCA 003268675.1 | 99.24 | 98.06 | 99.07 |
| *Streptomyces cavourensis* | 95.07 | GCA 006788935 | 99.72 | 97.97 | 99.07 |
| *Streptomyces fulvissimus* | 90.71 | GCA 000385945.1 | 99.31 | 94.69 | 98.45 |
| *Streptomyces parvus* | 89.14 | GCA 000702365.1 | 99.24 | 94.16 | 98.76 |
| *Streptomyces setonii* | 89.25 | GCA 002154345.1 | 99.17 | 94.16 | 99.53 |

ANI, average nucleotide identity.

**Table 3.** Antibacterial gene clusters prediction by antiSMASH, NCBI, and RAST annotation of *Streptomyces bacillais* S8 genome

| antiSMASH | | | NCBI | RAST |
|---|---|---|---|---|
| Type | Most similar known cluster | Similarity (%) | | |
| NRPS | Valinomycin | 86 | Nonribosomal peptide biosynthesis | Nonribosomal peptide biosynthesis |
| NRPS | Salinomycin | 14 | Nonribosomal peptide biosynthesis | Nonribosomal peptide biosynthesis |
| NRPS-like | Bottromycin A2 | 36 | Nonribosomal peptide biosynthesis | Nonribosomal peptide biosynthesis |
| T1PKS | Bafilomycin B1 | 94 | Polyketide biosynthesis | Polyketide biosynthesis |
| PKS-like | Cosmomycin D | 5 | Hypothetical protein | Hypothetical protein |
| Siderophore | Ficellomycin | 3 | Siderophore biosynthesis | Siderophore biosynthesis |
| Butyrolactone | Shodomycin | 47 | Hypothetical protein | Hypothetical protein |
| Butyrolactone | Coelimycin P1 | 16 | Hypothetical protein | ABC transpoter |
| Terpene | Steffimycin D | 19 | Hypothetical protein | Hypothetical protein |

coverage and 95.31% ANI similarity with *S. bacillaris* and also 16S rRNA, *recA,* and *rplC* genes sequences information matched with *S. bacillaris* at 98% similarity (Table 2). Accordingly, the *Streptomyces* sp. S8 was re-classified as *S. bacillaris* S8 (Fig. 6). Biocontrol approaches in plant disease management are highlighted with sustainable agriculture aspect, especially in the genus of *Streptomyces*, which produces various antibiotic compounds (Kim et al., 2019a, 2021a). *Streptomyces* sp. S8 was reported as a powerful biocontrol agent against the large patch disease of turfgrass (Jeon et al., 2019). The strain has one chromosome and a single plasmid; the chromosome predicted 9 antibacterial-related metabolite gene clusters by three independent annotation tools (Table 3). Among the 9 putative antibacterial metabolites, salinomycin, valinomycin, and bafilomycin were tested for their antibacterial ability with a plate assay. Only salinomycin showed antibacterial activity against *X. citri* pv. *glycine* (Fig. 5D-H). Salinomycin is known to have the effect of disturbing cell membranes (Dewangan et al., 2017). The result suggested that *S. bacillaris* S8 had dual antibiotic functions as valinomycin for antifungal and salinomycin for antibacterial activities. *S. bacillaris* S8 may have the advantage of developing as a commercial biological control product.

We observed and compared microbiota communities in *X. citri* pv. *glycine* infection or non-infection soybeans. At the infected plant, microbiota community structures were disrupted, and it caused a reduction of *Streptomyces* population in the community. The key strain associated with healthy soybean was identified as *S. bacillaris* S8. Genome analysis and *in vitro* antibacterial tests, an antibiotic produced by the S8, salinomycin inhibited *X. citri* pv. *glycine.* These results suggested that *Streptomyces* was the key microbe in the microbial community for healthy soybean and presented how microbiota structure studies can reveal the biocontrol agents.

## Conflicts of Interest

No potential conflict of interest relevant to this article was reported.

## Acknowledgments

This research was supported by an agenda research program by the Rural Development Administration (PJ015871).

## References

Aziz, R. K., Bartels, D., Best, A. A., DeJongh, M., Disz, T., Ed-

wards, R. A., Formsma, K., Gerdes, S., Glass, E. M., Kubal, M., Meyer, F., Olsen, G. J., Olson, R., Osterman, A. L., Overbeek, R. A., McNeil, L. K., Paarmann, D., Paczian, T., Parrello, B., Pusch, G. D., Reich, C., Stevens, R., Vassieva, O., Vonstein, V., Wilke, A. and Zagnitko, O. 2008. The RAST Server: rapid annotations using subsystems technology. *BMC Genomics* 9:75.

Bintarti, A. F., Sulesky-Grieb, A., Stopnisek, N. and Shade, A. 2022. Endophytic microbiome variation among single plant seeds. *Phytobiomes J*. 6:45-55.

Blin, K., Shaw, S., Kloosterman, A. M., Charlop-Powers, Z., van Wezel, G. P., Medema, M. H. and Weber, T. 2021. antiSMASH 6.0: improving cluster detection and comparison capabilities. *Nucleic Acids Res*. 49:W29-W35.

Callahan, B. J., McMurdie, P. J., Rosen, M. J., Han, A. W., Johnson, A. J. A. and Holmes, S. P. 2016. DADA2: high-resolution sample inference from Illumina amplicon data. *Nat. Methods* 13:581-583.

Chen, S., Chen, X. and Xu, J. 2016. Impacts of climate change on agriculture: evidence from China. *J. Environ. Econ. Manage*. 76:105-124.

Colombo, E. M., Kunova, A., Pizzatti, C., Saracchi, M., Cortesi, P. and Pasquali, M. 2019. Selection of an endophytic *Streptomyces* sp. strain DEF09 from wheat roots as a biocontrol agent *against Fusarium graminearum*. *Front. Microbiol*. 10:2356.

Dang, H., Zhang, T., Li, G., Mu, Y., Lv, X., Wang, Z. and Zhuang, L. 2020. Root-associated endophytic bacterial community composition and structure of three medicinal licorices and their changes with the growing year. *BMC Microbiol*. 20:291.

de Almeida Lopes, K. B., Carpentieri-Pipolo, V., Oro, T. H., Stefani Pagliosa, E. and Degrassi, G. 2016. Culturable endophytic bacterial communities associated with field-grown soybean. *J. Appl. Microbiol*. 120:740-755.

Deng, S., Caddell, D. F., Xu., G., Dahlen, L., Washington, L., Yang, J. and Coleman-Derr, D. 2021. Genome wide association study reveals plant loci controlling heritability of the rhizosphere microbiome. *ISME J.* 15:3181-3194.

Dewangan, J., Srivastava, S. and Rath, S. K. 2017. Salinomycin: a new paradigm in cancer therapy. *Tumour Biol.* 39:1010428317695035.

Dini-Andreote, F. and Raaijmakers, J. M. 2018. Embracing community ecology in plant microbiome research. *Trends Plant Sci*. 23:467-469.

Dong, L., Cheng, R., Xiao, L., Wei, F., Wei, G., Xu, J., Wang, Y., Guo, X., Chen, Z. and Chen, S. 2018. Diversity and composition of bacterial endophytes among plant parts of *Panax notoginseng. Chin. Med.* 13:41.

Han, Q., Ma, Q., Chen, Y., Tian, B., Xu, L., Bai, Y., Chen, W. and Li, X. 2020. Variation in rhizosphere microbial communities and its association with the symbiotic efficiency of rhizobia in soybean. *ISME J*. 14:1915-1928.

Hannula, S. E., Zhu, F., Heinen, R. and Bezemer, T. M. 2019. Foliar-feeding insects acquire microbiomes from the soil rather than the host plant. *Nat. Commun*. 10:1254.

Hwang, H.-H., Chien, P.-R., Huang, F.-C., Hung, S.-H., Kuo, C.-H., Deng, W.-L., Chiang, E.-P. I. and Huang, C.-C. 2021. A plant endophytic bacterium, *Burkholderia seminalis* strain 869T2, promotes plant growth in Arabidopsis, Pak Choi, Chinese Amaranth, Lettuces, and other vegetables. *Microorganisms* 9:1703.

Ikeda, S., Rallos, L. E. E., Okubo, T., Eda, S., Inaba, S., Mitsui, H. and Minamisawa, K. 2008. Microbial community analysis of field-grown soybeans with different nodulation phenotypes. *Appl. Environ. Microbiol.* 74:5704-5709.

Jägermeyr, J., Robock, A., Elliott, J., Müller, C., Xia, L., Khabarov, N., Folberth, C., Schmid, E., Liu, W., Zabel, F., Rabin, S. S., Puma, M. J., Heslin, A., Franke, J., Foster, I., Asseng, S., Bardeen, C. G., Toon, O. B. and Rosenzweig, C. 2020. A regional nuclear conflict would compromise global food security. *Proc. Natl. Acad. Sci. U. S. A.* 117:7071-7081.

Jeon, C.-W., Kim, D.-R. and Kwak, Y.-S. 2019. Valinomycin, produced by *Streptomyces* sp. S8, a key antifungal metabolite in large patch disease suppressiveness. *World J. Microbiol. Biotechnol.* 35:128.

Jeong, N., Kim, K.-S., Jeong, S., Kim, J.-Y., Park, S.-K., Lee, J. S., Jeong, S.-C., Kang, S.-T., Ha, B.-K., Kim, D.-Y., Kim, N., Moon, J.-K. and Choi, M. S. 2019. Korean soybean core collection: genotypic and phenotypic diversity population structure and genome-wide association study. *PLoS ONE* 14:e0224074.

Kang, I.-J., Kim, K. S., Beattie, G. A., Chung, H., Heu, S. and Hwang, I. 2021. Characterization of *Xanthomonas citri* pv. *glycines* population genetics and virulence in a national survey of bacterial pustule disease in Korea. *Plant Pathol. J*. 37:652-661.

Kruskal, W. H. and Wallis, W. A. 1952. Use of ranks in one-criterion variance analysis. *J. Am. Stat. Assoc*. 47.260:583-621.

Kim, D.-R., Cho, G., Jeon, C.-W., Weller, D. M., Thomashow, L. S., Paulitz, T. C. and Kwak, Y.-S. 2019a. A mutualistic interaction between *Streptomyces* bacteria, strawberry plants and pollinating bees. *Nat. Commun*. 10:4802.

Kim, D.-R., Jeon, C.-W., Cho, G., Thomashow, L. S., Weller, D. M., Paik, M.-J., Lee, Y. B. and Kwak, Y.-S. 2021a. Glutamic acid reshapes the plant microbiota to protect plants against pathogens. *Microbiome* 9:244.

Kim, D.-R. and Kwak, Y.-S. 2021. A genome-wide analysis of antibiotic producing genes in *Streptomyces globisporus* SP6C4. *Plant Pathol. J.* 37:389-395.

Kim, M.-J., Chae, D.-H., Cho, G., Kim, D.-R. and Kwak, Y.-S. 2019b. Characterization of antibacterial strains against kiwifruit bacterial canker pathogen. *Plant Pathol. J.* 35:473-485.

Kim, S.-H., Cho, G., Lee, S. I., Kim, D.-R. and Kwak, Y.-S. 2021b. Comparison of bacterial community of healthy and *Erwinia amylovora* infected apples. *Plant Pathol. J.* 37:396-403.

Lau, J. A., Lennon, J. T. and Heath, K. D. 2017. Trees harness the power of microbes to survive climate change. *Proc. Natl. Acad. Sci. U. S. A.* 114:11009-11011.

Longley, R., Noel, Z. A., Benucci, G. M. N., Chilvers, M. I., Trail, F. and Bonito, G. 2020. Crop management impacts the soybean (*Glycine max*) microbiome. *Front. Microbiol*. 11:1116.

Lopez-Velasco, G., Carder, P. A., Welbaum, G. E. and Ponder, M. A. 2013. Diversity of the spinach (*Spinacia oleracea*) spermosphere and phyllosphere bacterial communities. *FEMS Microbiol. Lett.* 346:146-154.

Lundberg, D. S., Yourstone, S., Mieczkowski, P., Jones, C. D. and Dangl, J. L. 2013. Practical innovations for high-throughput amplicon sequencing. *Nat. Methods* 10:999-1002.

Lu, T., Ke, M., Lavoie, M., Jin, Y., Fan, X., Zhang, Z., Fu, Z., Sun, L., Gillings, M., Peñuelas, J., Qian, H. and Zhu, Y.-G. 2018. Rhizosphere microorganisms can influence the timing of plant flowering. *Microbiome* 6:231.

Mingma, R., Pathom-aree, W., Trakulnaleamsai, S., Thamchaipenet, A. and Duangmal, K. 2014. Isolation of rhizospheric and roots endophytic actinomycetes from Leguminosae plant and their activities to inhibit soybean pathogen, *Xanthomonas campestris* pv. *glycine*. *World J. Microbiol. Biotechnol.* 30:271-280.

Murali, A., Bhargava, A. and Wright, E. S. 2018. IDTAXA: a novel approach for accurate taxonomic classification of microbiome sequences. *Microbiome* 6:140.

Orozco-Mosqueda, M. D. C. and Santoyo, G. 2021. Plant-microbial endophytes interactions: scrutinizing their beneficial mechanisms from genomic explorations. *Curr. Plant Biol*. 25:100189.

Park, D. S., Kim, J. S., Han. C. H., Ko, S. J. and Kim, H. K. 2007. (Korea) The primer set for sensitive and specific detection of *Xanthomonas axonopodis* pv. *glycines* by polymerase chain reaction. KB101834763B1. 9 May 2007.

Reverchon, F. and Méndez-Bravo, A. 2021. Plant-mediated above-belowground interactions: a phytobiome story. In: *Plant-animal interactions: source of biodiversity*, eds. by K. Del-Claro and H. M. Torezan-Sillingardi, pp. 205-231. Springer, Cham, Switzerland.

Rodriguez, R. and Durán, P. 2020. Natural holobiome engineering by using native extreme microbiome to counteract the climate change effects. *Front. Bioeng. Biotechnol*. 8:568.

Simonin, M., Briand, M., Chesneau, G., Rochefort, A., Marais, C., Sarniguet, A. and Barret, M. 2022. Seed microbiota revealed by a large-scale meta-analysis including 50 plant species. *New Phytol*. 234:1448-1463.

Teeling, H. and Glöckner, F. O. 2012. Current opportunities and challenges in microbial metagenome analysis: a bioinformatic perspective. *Brief Bioinform.* 13:728-742.

Teheran-Sierra, L. G., Funnicelli, M. I. G., de Carvalho, L. A. L., Ferro, M. I. T., Soares, M. A. and Pinheiro, D. G. 2021. Bacterial communities associated with sugarcane under different agricultural management exhibit a diversity of plant growth-promoting traits and evidence of synergistic effect. *Microbiol. Res.* 247:126729.

Villalobos, J. A., Yi, B. R. and Wallace, I. S. 2015. 2-Fluoro-L-fucose is a metabolically incorporated inhibitor of plant cell wall polysaccharide fucosylation. *PLoS ONE* 10:e0139091.

Wilson, K. 2001. Preparation of genomic DNA from bacteria. *Curr. Protoc. Mol. Biol.* 56:2.4.

Xiong, C., Singh, B. K., He, J.-Z., Han, Y.-L., Li, P.-P., Wan, L.-H., Meng, G.-Z., Liu, S.-Y., Wang, J.-T., Wu, C.-F., Ge, A.-H. and Zhang, L.-M. 2021. Plant developmental stage drives the differentiation in ecological role of the maize microbiome. *Microbiome* 9:171.

Xu, T., Cao, L., Zeng, J., Franco, C. M. M., Yang, Y., Hu, X., Liu, Y., Wang, X., Gao, Y., Bu, Z., Shi, L., Zhou, G., Zhou, Q., Liu, X. and Zhu, Y. 2019a. The antifungal action mode of the rice endophyte *Streptomyces hygroscopicus* OsiSh-2 as a potential biocontrol agent against the rice blast pathogen. *Pestic. Biochem. Physiol*. 160:58-69.

Xu, Y., Ge, Y., Song, J. and Rensing, C. 2019b. Assembly of root-associated microbial community of typical rice cultivars in different soil types. *Biol. Fertil. Soils* 56:249-260.

Yoon, S.-H., Ha, S.-M., Kwon, S., Lim, J., Kim, Y., Seo, H. and Chun, J. 2017. Introducing EzBioCloud: a taxonomically united database of 16S rRNA gene sequences and whole-genome assemblies. *Int. J. Syst. Evol. Microbiol*. 67:1613-1617.